

Multi-length scale design of deformation processes for control of orientation (texture) dependent properties

Shankar Ganapathysubramanian* and Nicholas Zabaras*

**Materials Process Design and Control Laboratory, Sibley School of Mechanical and Aerospace Engineering, 188 Frank H. T. Rhodes Hall, Cornell University Ithaca, NY 14853-3801, USA*

Abstract. Design of deformation (thermo-mechanical) processes to achieve desired structural response will be addressed. Plastic deformation is assumed to be accommodated through crystallographic slip and reorientation of crystals. Conventional methodologies towards polycrystal plasticity use an aggregate of single crystals and this choice of the aggregate affects the response of the polycrystal. In order to address this issue, a continuum approach will be presented for the representation of polycrystals through an orientation distribution function over the orientation space. In addition, conventional polycrystal plasticity models do not consider strain rate and temperature effects on the mechanical response of a crystal. In this effort, a constitutive framework for thermo-elastic-viscoplastic response will be described along with a coupled macro-micro, fully implicit algorithm [1]. Numerical examples that highlight the benefits of the proposed approach will be detailed. Design/control problems, relevant to industry, and involving microstructure sensitive-design of processes will be addressed. A novel, coupled macro-micro continuum sensitivity analysis [2] has been developed for the thermo-mechanical deformation process and is used in a gradient based optimization framework [3]. The design problems are posed as optimization problems with design variables chosen to characterize macro-scale deformation. Through these complex examples, we aim to show that accurate modeling and control of microstructure-sensitive material response is indeed feasible.

1. INTRODUCTION

The use of computer technology for simulation of deformation processes has increased substantially over the last 30 years. One of the major developments during this period has been the modeling of behavior of crystalline materials using coupled length scale models. Even though most materials are crystalline, many approaches to the design of deformation processes of polycrystal materials assume the material to be isotropic using modeling and control algorithms that are based on phenomenological microstructure evolution constitutive models [4]. However, most process design applications are quite sensitive to the anisotropy of these crystalline materials. Process optimization is especially important for hardware components in critical applications in the aerospace, naval and automotive industries where there is a permanent need to reduce material utilization for reduced process cost, fuel consumption and higher mobility. In addition, such critical components require performance specifications that are directly related to the microstructure obtained during processing. This calls for a direct coupling between material microstructural features and the performance required from the application for which the material will be used. Very little attention has been devoted to controlling texture to obtain desired microstructural properties. The only notable work is on the design of a compliant fixed guided beam with the microstruc-

ture being represented as a design variable using spectral methods [5]. The concentration of this paper is on developing a material point design simulator that can be used to control texture-dependent material properties. This can be considered as the first step towards the development of a multi-scale virtual environment where it would be possible to design the process sequence and the macroscopic process parameters in order to obtain desired microstructure-sensitive properties in the product.

2. CONTINUUM MICROSTRUCTURE REPRESENTATION

Anisotropy is primarily due to the crystallographic texture, which can be defined as a preferred orientation of the crystals in a particular direction. The state of art in simulation of texture evolution is based on the analysis of a discrete aggregate of crystals [6]. This approach combines single crystal responses with a macro-micro linking hypothesis. Recent work in the field of texture analysis and modeling has concentrated on representation of texture evolution by an orientation distribution function (ODF). The ODF represents the probability density of finding a crystal orientation within the three-dimensional orientation space. A finite element representation of the ODF using angle-axis parametrization has been used.

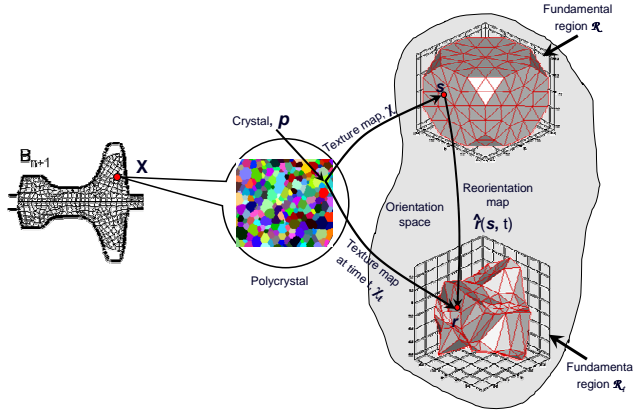


FIGURE 1. A framework for the association of a crystal \mathbf{p} with unique parameters r , drawn from the fundamental region.

Angle-axis representations define an alternative way of representing texture compared to the use of Euler angles. Any orientation can be uniquely represented by a rotation about an axis (represented by a unit vector \mathbf{n}) by an angle. More details about these representations can be obtained from [7, 8]. Texture, from [7], can be described as a map that takes individual crystals, \mathbf{p} , to orientations within the fundamental region. The orientation of a crystal r is then developed as $r = \chi(\mathbf{p})$, where χ is the texture map. A graphical representation of this framework is shown in Fig. 1. The microstructure is thus treated as a continuum of crystals, that under the map χ occupies the fundamental region, \mathcal{R} . The reorientation vector, \hat{r} is integral to this analysis and is defined in [7]. The reorientation velocity can be evaluated as:

$$\mathbf{v} = \frac{1}{2}(\boldsymbol{\omega} + (\boldsymbol{\omega} \cdot \mathbf{r})\mathbf{r} + \boldsymbol{\omega} \times \mathbf{r}) \quad (1)$$

where $\boldsymbol{\omega}$ represents the spin vector, defined as $\boldsymbol{\omega} = \text{vect}(\dot{R}R^T) = \text{vect}(\boldsymbol{\Omega})$. The Lagrangian version of the ODF conservation equation is [7]:

$$\hat{\mathcal{A}}(s,t)J(s,t) = \hat{\mathcal{A}}(s,0) = \mathcal{A}_0(s) \quad (2)$$

where $J(s,t) = \det(\nabla \hat{r}(s,t))$, $\hat{\mathcal{A}}(s,t)$ is Lagrangian description of the ODF (at a reference orientation s) and $\mathcal{A}_0(s)$ is the initial texturing of the material. Consider a polycrystal average of an orientation dependent property, $\Upsilon(r,t)$, that is determined as:

$$\langle \Upsilon \rangle = \int_{\mathcal{R}} \Upsilon(r,t) \mathcal{A}(r,t) dv = \int_{\mathcal{R}_0} \Upsilon(\hat{r}(s,t),t) \mathcal{A}_0(s) dv_0 \quad (3)$$

Thus from Equation (3), one can conclude that if the reorientation and the initial texturing are known, then the average property for the polycrystal is also known. The interested reader is referred to [8] for a detailed description of the advantages of these methods.

3. SOLVING THE DIRECT DEFORMATION PROBLEM

The direct deformation problem can be stated as follows: Compute the time history of deformation, temperature and material state of a workpiece made of a polycrystal material deforming as a result of external forces and/or deformation due to contact and friction at the workpiece-die interface. Let \mathcal{B}_0 be the initial configuration of the body (at time $t = 0$) and \mathcal{B}_{n+1} the current configuration at time t . The total deformation gradient is then defined as: $F(X,t) = \nabla_0 \phi(X,t) = \frac{\partial \phi(X,t)}{\partial X}$, $\det F > 0$, where ϕ represents the deformation map from \mathcal{B}_0 to \mathcal{B}_{n+1} (Fig. 2). Furthermore, using the extended Taylor assumption, the deformation gradient on a crystal is equal to the macroscopic deformation gradient. The average response of a polycrystal is obtained by computing a weighted average of the single crystal response over the fundamental region (Equation (3)). Thus the constitutive problem is solved at each point of the reference fundamental region. A total Lagrangian framework is adopted in this effort. The equilibrium equation can be expressed in this framework as $\nabla_0 \cdot \langle P \rangle + f = 0$, where $\nabla_0 \cdot$ represents the divergence on the reference configuration. The polycrystal average of the PK-I stress is computed as, $\langle P \rangle = \det F \langle T \rangle F^{-T}$ where $\langle T \rangle$ is the polycrystal Cauchy stress. The weak form of this equation, for any kinematically admissible test function \tilde{u} , can be written:

$$\mathcal{G}(u_{n+1}, \tilde{u}) \equiv \int_{\mathcal{B}_0} \langle P \rangle \bullet \nabla_0 \tilde{u} dV - \int_{\partial \mathcal{B}_0} \lambda \bullet \tilde{u} dA - \int_{\mathcal{B}_0} f \bullet \nabla_0 \tilde{u} dV = 0 \quad (4)$$

where the applied surface traction λ and body forces f are given. We make a simplifying assumption that the contact problem is independent of the nature of the underlying microstructure, and that texture plays a role only through the stress response. To solve this non-linear equation, a Newton-Raphson iterative scheme along with a line search procedure is employed. A linearization is necessary as part of this solution process and [1, 9] clearly outline the linearization process for the constitutive and contact sub-problems respectively. The solution of the thermal problem is described in [10].

4. CRYSTAL CONSTITUTIVE MODEL

During a deformation process, crystallographic slip and reorientation of crystals are assumed to be the primary mechanisms of plastic deformation. At absolute zero, the slip resistance $s^\alpha(0)$, of slip system α has to be completely overcome by the resolved stress, τ^α (defined in [1]). At temperatures $> 0K$, short-range obstacles can be overcome at a lower stress level with the help of the addi-

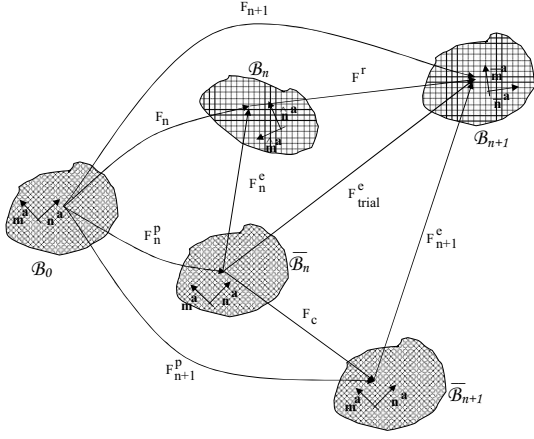


FIGURE 2. Evolution of various material configurations for a single crystal as needed in the integration of the constitutive model. Here m denotes the slip direction and n denotes the slip normal, which together define the slip systems and are assumed to be known on the reference (initial) configuration. Further, the Schmid tensor is evaluated as $S_0 = m \otimes n$.

tional thermal energy. Obstacles can therefore be classified as thermal and athermal [11]. In metals without large precipitates, since it is known that the thermal energy is sufficient to overcome short range barriers, the constitutive formulations are expressed in terms of the thermal part of the resolved shear stress and the thermal part of the shearing resistance. Such a formulation is detailed in [1] and forms the basis of the present study. The total deformation gradient is decomposed into plastic and elastic parts as (Fig. 2) $F = F^e F^p$ where F^e and F^p are the elastic and plastic deformation gradients, with $\det F^p = 1$. The evolution of the plastic flow is given by

$$\dot{F}^p (F^p)^{-1} = \sum_{\alpha} \dot{\gamma}^{\alpha} S_0^{\alpha} \quad (5)$$

where $S_0^{\alpha} = m_0^{\alpha} \otimes n_0^{\alpha}$ is the Schmid tensor and $\dot{\gamma}^{\alpha}$ is the plastic shearing rate on the α^{th} slip system. Fig. 2 clearly describes the constitutive problem along with the slip systems in different configurations. An Euler-backward time integration procedure leads to the following approximation, $F^p = \exp(\Delta t \sum_{\alpha} \dot{\gamma}^{\alpha} S_0^{\alpha}) F_n^p \approx (I + \Delta t \sum_{\alpha} \dot{\gamma}^{\alpha} S_0^{\alpha}) F_n^p$. Simple manipulation of this equation, along with a Green elastic strain measure (defined on the relaxed configuration $\bar{\mathcal{B}}$), results in the following:

$$\bar{E}^e = \frac{1}{2} (F^{eT} F^e - I) = \bar{E}_{trial}^e - \frac{\Delta t}{2} \sum_{\alpha} \dot{\gamma}^{\alpha} ((S_0^{\alpha})^T (F_{trial}^e)^T F_{trial}^e + (F_{trial}^e)^T F_{trial}^e S_0^{\alpha}) \quad (6)$$

where $\bar{E}_{trial}^e = \frac{1}{2} ((F_{trial}^e)^T F_{trial}^e - I)$ and F_{trial}^e is the trial elastic deformation gradient given as $F_{n+1} (F_n^p)^{-1}$. The

corresponding conjugate stress measure is defined as

$$\bar{T} = \det F^e (F^e)^{-1} T (F^e)^{-T} \quad (7)$$

where T is the Cauchy stress for the crystal. The constitutive relation for small temperature changes about the initial temperature, θ_0 , is given as

$$\bar{T} = \mathcal{L}^e [\bar{E}^e - A(\theta - \theta_0)] \quad (8)$$

where \mathcal{L}^e is the fourth-order anisotropic elasticity tensor and A is the second-order anisotropic thermal expansion tensor. Further, the resolved shear stress and slip system resistance are considered as $s^{\alpha} = s_{at}^{\alpha} + s_t^{\alpha}$; $\tau_t^{\alpha} = |\tau^{\alpha}| - s_{at}^{\alpha}$ where the subscripts t and at denote the thermal and athermal parts, respectively. τ^{α} , the resolved shear stress, is computed as $\bar{T} \bullet S_0^{\alpha}$. The shearing rate is given by the power law:

$$\dot{\gamma}^{\alpha} = \begin{cases} 0, \tau_t^{\alpha} \leq 0 \\ \dot{\gamma}_0 \exp\left\{-\frac{\Delta G^{\alpha}}{k_B \theta}\right\} \text{sign}(\tau^{\alpha}), 0 < \tau_t^{\alpha} < s_t^{\alpha} \end{cases} \quad (9)$$

where, the activation enthalpy is given by $\Delta G^{\alpha} = \Delta F^{\alpha} \left[1 - \left\{\frac{\tau_t^{\alpha}}{s_t^{\alpha}}\right\}^p\right]^q$. Furthermore, the slip system resistances s_{at}^{α} and s_t^{α} evolve with deformation as

$$s^{\alpha} = \sum_{\beta} h^{\alpha\beta} |\dot{\gamma}^{\beta}| \quad (10)$$

with $h^{\alpha\beta}$ defined in [1, 11]. Special conditions for f.c.c and b.c.c materials and the procedure for the evaluation of the resolved shear stress τ^{α} and the slip system resistance s^{α} are also discussed in [1]. In addition, $\omega = \text{vect}(\Omega)$ is evaluated from $\frac{1}{\Delta t} \ln(R_{n+1} R_n^T)$, and R is evaluated from the polar decomposition of the elastic deformation gradient as $F^e = R U^e$. To conclude this section, the average Cauchy stress is evaluated as

$$\langle T \rangle = \int_{\mathcal{R}_0} T(\hat{r}(s, t), t) \mathcal{A}_0(s) dv_0 \quad (11)$$

5. DEFINITION OF PARAMETER SENSITIVITY

The design framework adopted here is based on a gradient optimization method. To calculate the gradients, the sensitivity of material properties with respect to macro-design variables needs to be evaluated. The process of evaluating the sensitivities of fields on the micro-scale due to perturbations on the macro-scale is shown schematically in Fig. 3. This requires a macro-sensitivity problem where the interest is to compute how perturbations on the macro-design variables β affect the continuum fields including the deformation and velocity gradients, F , L respectively. The macro-sensitivity problem

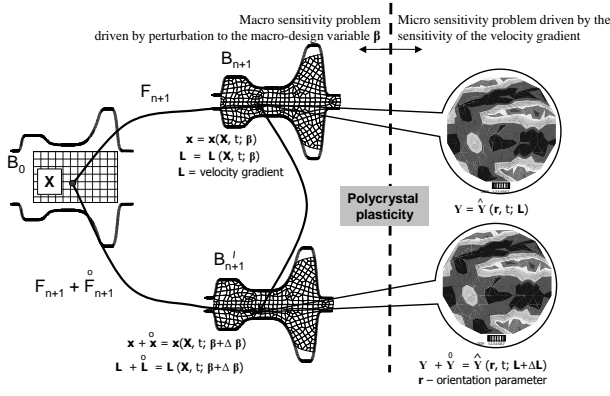


FIGURE 3. Pictorial of the two-length scale sensitivity analysis. On the left, the macro-sensitivity problem computes the sensitivities of continuum fields (e.g. of the deformation gradient) with respect to macro-design variables. On the right, the micro-sensitivity problem computes the sensitivity of the material properties related to the ODF.

is examined in [3, 4, 7] and the reader is encouraged to consult these references for more details. Parameter sensitivity of a generic field Y expressed in a total Lagrangian (TL) framework is briefly described. Detailed information can be obtained from [3]. Sensitivities of the deformation or material state are quantitative measures of changes in the deformation and material state as a result of infinitesimal perturbations to process parameters β (parameter sensitivity). The dependence of the TL field on β can be expressed as $Y = \tilde{Y}(X, r, t; \beta)$, where X is on the reference configuration, and r is the current crystal orientation. Thus the parameter sensitivity $\dot{Y} = \dot{Y}(X, r, t; \beta, \Delta\beta)$ is defined as the total Gateaux differential of $Y = \tilde{Y}(X, r, t; \beta)$ in the direction $\Delta\beta$ computed at β

$$\tilde{\dot{Y}}(X, r, t; \beta, \Delta\beta) = \left. \frac{d}{d\lambda} \tilde{Y}(X, r, t; \beta + \lambda\Delta\beta) \right|_{\lambda=0} \quad (12)$$

6. DEFORMATION SENSITIVITY PROBLEM

The salient feature of this work is that equations governing the sensitivity fields are computed at the continuum level. The equilibrium equation is considered and ‘design differentiated’. This continuum, differential, sensitivity equilibrium equation is then posed in a weak form so as to establish a principle of virtual work like equation for the calculation of the sensitivity of deformation fields [10]. Consistent with this mode of analysis, the sensitivity constitutive, sensitivity thermal and sensitivity con-

tact equations are derived from their corresponding continuum equations rather than their numerically integrated counterparts. Described below is the analysis for a total Lagrangian formulation with emphasis on the constitutive aspects of the problem. For completeness, we briefly review the kinematic sensitivity problem. The deformation sensitivity problem is developed on the reference configuration \mathcal{B}_0 . The design differentiation of the equilibrium

results in $\overline{\nabla_0 \cdot \langle P \rangle} + \dot{f} = \mathbf{0}, \forall X \in \mathcal{B}_0, \forall t \in [0, t_f]$, where $\langle P \rangle$ is the polycrystal averaged PK-I stress defined earlier. A variational form for the sensitivity equilibrium equation (for parameter sensitivity) can be posed as follows: Evaluate $\dot{x} = \dot{x}(X, t; \beta, \Delta\beta)$ such that

$$\int_{\mathcal{B}_0} \langle P \rangle \cdot \nabla_0 \tilde{\eta} dV_0 = \int_{\partial\mathcal{B}_0} \dot{\lambda} \cdot \tilde{\eta} dA_0 \quad (13)$$

for every $\tilde{\eta}$, a kinematically admissible sensitivity deformation field expressed over the reference configuration \mathcal{B}_0 . In order to solve the weak form defined by equation

Equation (13), relationships between (a) \dot{F} and \dot{x} (b) $\langle P \rangle$ and $[\dot{F}, \dot{\theta}]$ and (c) $\dot{\lambda}$ and \dot{x} need to be developed. The relationship between \dot{F} and \dot{x} is purely kinematic and the relationship between $\langle P \rangle$ and $[\dot{F}, \dot{\theta}]$ is obtained from the sensitivity constitutive problem to be discussed in section 7 and takes the form:

$$\langle P \rangle = \mathcal{B} [\dot{F}] + C \dot{\theta} + G \quad (14)$$

where \mathcal{B} is a fourth order tensor and C, G are second order tensors. These tensors, are constants, defined from known direct and sensitivity fields at the previous time step, and are obtained by considering the polycrystal average of each crystal response (see section 7). The relationship between $\dot{\lambda}$ and \dot{x} is obtained from the sensitivity contact problem as $\dot{\lambda} = H[\dot{x}] + d$, where H is a second order tensor and d a vector. The non-trivial derivation of these tensors resulting by design-differentiation of a regularized contact problem can be found in [9].

7. SENSITIVITY CONSTITUTIVE PROBLEM

Through the crystal constitutive sensitivity sub-problem, the relationship between the polycrystal average, $\langle T \rangle$ and $[\dot{F}, \dot{\theta}]$ is computed. As part of the update procedure, one computes the set $\{\dot{T}, \dot{s}, \dot{\tau}, \dot{F}^e, \dot{F}^p\}$ for each crystal orientation at the end of the time increment t_{n+1} where the sensitivity of the total deformation gradient \dot{F}_{n+1} and

the sensitivity of the temperature field $\overset{\circ}{\theta}_{n+1}$ are assumed known. The polycrystal average of the sensitivity $\overset{\circ}{\mathcal{W}}_{mech}$ of the mechanical dissipation \mathcal{W}_{mech} is also computed as being a driving force for the thermal sensitivity problem at time t_{n+1} (refer to [1, 2]). The solution of the direct thermo-mechanical problem is known at time t_{n+1} , the body configuration \mathcal{B}_{n+1} as well as the temperature field θ_{n+1} are known at t_{n+1} . The constitutive sensitivity problem for a crystal orientation is history dependent and the solution of the sensitivity problem at time t_n is assumed known for each crystal orientation, yielding the variables $\{\overset{\circ}{T}, \overset{\circ}{s}, \overset{\circ}{\tau}, \overset{\circ}{F}^e, \overset{\circ}{F}^p\}$ at the beginning of each time increment. This methodology follows and uses ideas from earlier publications like [3, 4, 10], and the reader is referred to these for additional details not available in this development. It was also shown that the deformation sensitivity response is dependent only on the instantaneous temperature sensitivity response $\overset{\circ}{\theta}_{n+1}$.

7.1. Calculation of a linear relation between $\overset{\circ}{s}$ and $[\overset{\circ}{T}_{n+1}, \overset{\circ}{\theta}_{n+1}]$

Consider the design-differentiation of the evolution equation for the deformation resistance, s . Euler-backward integration results in:

$$\begin{aligned} \overset{\circ}{s}_{n+1} - \Delta t \sum_{\beta} q^{\alpha\beta} \frac{\partial g^{\beta}}{\partial s^{\beta}} \overset{\circ}{s}_{n+1} &= \overset{\circ}{s}_n + \\ \Delta t \sum_{\beta} q^{\alpha\beta} \frac{\partial g^{\beta}}{\partial \tau^{\beta}} \overset{\circ}{\tau}_{n+1} + \Delta t \sum_{\beta} q^{\alpha\beta} \frac{\partial g^{\beta}}{\partial \theta} \overset{\circ}{\theta}_{n+1} &(15) \end{aligned}$$

Rearranging the above set of equations results in:

$$\overset{\circ}{s}_{n+1} = \sum_{\beta} m^{\alpha\beta} \overset{\circ}{\tau}^{\beta} + v_1^{\alpha} \overset{\circ}{\theta} + v_2^{\alpha} \quad (16)$$

where $m^{\alpha\beta}$, v_1^{α} and v_2^{α} are constants. It is further known that $\tau^{\beta} = \overset{\circ}{T} \cdot S_0^{\alpha}$; design-differentiation of this relation results in $\overset{\circ}{\tau}^{\beta} = \overset{\circ}{T} \cdot S_0^{\alpha}$. Substituting this relation into Equation (16) results in the following:

$$\{\overset{\circ}{s}_{n+1}\} = \left[\frac{Ds}{D\tau} \right] : \overset{\circ}{T} + \{v_1\} \overset{\circ}{\theta} + \{v_2\} \quad (17)$$

where $\left[\frac{Ds}{D\tau} \right]$ is a 3^{rd} order tensor and v_1, v_2 are vectors.

7.2. Calculation of a linear relation between $\overset{\circ}{F}_{n+1}^p$ and $[\overset{\circ}{T}_{n+1}, \overset{\circ}{\theta}_{n+1}]$

The evolution equation for $\overset{\circ}{F}^p$ is evaluated as:

$$\frac{\partial \overset{\circ}{F}^p}{\partial t} = \overset{\circ}{L}^p \overset{\circ}{F}^p + \overset{\circ}{\tilde{L}}^p \overset{\circ}{F}^p \quad (18)$$

where $\overset{\circ}{\tilde{L}}^p = \sum_{\alpha} \left[\overset{\circ}{\gamma}^{\alpha} S_0^{\alpha} \right]$ can be computed as,

$$\overset{\circ}{L}^p = \sum_{\alpha} \left[\frac{\partial \overset{\circ}{\gamma}^{\alpha}}{\partial \tau^{\alpha}} \overset{\circ}{\tau}^{\alpha} + \frac{\partial \overset{\circ}{\gamma}^{\alpha}}{\partial s^{\alpha}} s^{\alpha} + \frac{\partial \overset{\circ}{\gamma}^{\alpha}}{\partial \theta} \overset{\circ}{\theta} \right] S_0^{\alpha} \quad (19)$$

Euler-backward integration of Equation (18), with Equations (17), (19) and the definition of $\overset{\circ}{\tau}$ results in the following:

$$\overset{\circ}{F}_{n+1}^p (F_{n+1}^p)^{-1} = E + \mathcal{F} \left[\overset{\circ}{T}_{n+1} \right] + G \overset{\circ}{\theta}_{n+1} \quad (20)$$

where E, G are constant second tensors and \mathcal{F} is a fourth tensor. Furthermore, $\overset{\circ}{T}_{n+1}$ is related to $\overset{\circ}{F}_{n+1}^e$ and $\overset{\circ}{\theta}_{n+1}$ as:

$$\overset{\circ}{T} = \left(\frac{\partial \mathcal{L}^e}{\partial \theta} \right) [\overset{\circ}{E}^e] \overset{\circ}{\theta} + \mathcal{L}^e \left[\text{Sym} \left(F^{eT} \overset{\circ}{F}^e \right) \right] \quad (21)$$

where \mathcal{L}^e , the fourth-order anisotropic elasticity tensor, is assumed to be a function of temperature only. Using Equations (20) and (21), one can further obtain $\overset{\circ}{F}_{n+1}^p (F_{n+1}^p)^{-1}$ as a function of $\overset{\circ}{F}_{n+1}^e$.

7.3. Calculation of the linear relation between $\overset{\circ}{F}_{n+1}^e$ and $[\overset{\circ}{F}_{n+1}, \overset{\circ}{\theta}_{n+1}]$

Starting from the multiplicative decomposition of the deformation gradient, one can write $\overset{\circ}{F}_{n+1} = \overset{\circ}{F}_{n+1}^e F_{n+1}^p + F_{n+1}^e \overset{\circ}{F}_{n+1}^p$, which can then be simplified to [10],

$$(F_{n+1}^e)^{-1} \left(\overset{\circ}{F}_{n+1} F_{n+1}^{-1} \right) F_{n+1}^e = (F_{n+1}^e)^{-1} \overset{\circ}{F}_{n+1} + \overset{\circ}{F}_{n+1}^p (F_{n+1}^p)^{-1} \quad (22)$$

Substitution of the linear relationship between $\overset{\circ}{F}_{n+1}^p$ and $[\overset{\circ}{F}_{n+1}^e, \overset{\circ}{\theta}_{n+1}]$ results in the desired linear relationship:

$$\overset{\circ}{F}_{n+1}^e = \mathcal{C} (V_{n+1}) \left[\overset{\circ}{F}_{n+1} \right] + H \left(V_{n+1}, \overset{\circ}{V}_n \right) + M (V_{n+1}) \overset{\circ}{\theta}_{n+1} \quad (23)$$

where H and M are known second order tensor functions and \mathcal{C} , a known fourth order tensor function. The relationship between $\overset{\circ}{T}_{n+1}$ and $[\overset{\circ}{F}_{n+1}, \overset{\circ}{\theta}_{n+1}]$ is [10]

$$\begin{aligned} \overset{\circ}{T} &= - \frac{\text{tr} \left(\overset{\circ}{F}^e (F^e)^{-1} \right)}{\det(F^e)} T + \frac{1}{\det(F^e)} \overset{\circ}{F}^e \overset{\circ}{T} F^{eT} \\ &+ \frac{1}{\det(F^e)} F^e \overset{\circ}{T} F^{eT} + \frac{1}{\det(F^e)} F^e \overset{\circ}{T} \overset{\circ}{F}^{eT} \quad (24) \end{aligned}$$

Substitution of the linear relation between $\overset{\circ}{F}_{n+1}^e$ and $[\overset{\circ}{F}_{n+1}, \overset{\circ}{\theta}_{n+1}]$ in Equation (24), results in a linear relation between $\overset{\circ}{T}_{n+1}$ and $[\overset{\circ}{F}_{n+1}, \overset{\circ}{\theta}_{n+1}]$.

The previous sub-sections dealt with finding relations between different sensitivity terms for a given crystal orientation. This analysis has to be performed at all possible orientations to compute the polycrystal average. Consider, for example, the sensitivity of PK-I stress:

$$\langle \overset{\circ}{P} \rangle = \text{tr} \left(\overset{\circ}{F} \overset{\circ}{F}^{-1} \right) \det F \langle T \rangle F^{-T} + \det F \langle \overset{\circ}{T} \rangle F^{-T} - \det F \langle T \rangle F^{-T} \overset{\circ}{F} F^{-T} \quad (25)$$

where $\langle \overset{\circ}{T} \rangle = \int_{\mathcal{R}_0} \overset{\circ}{T} \mathcal{A}_0 dv$ and $\overset{\circ}{T}$ is described by the relations developed earlier. From these equations, one can generate the constants in Equation (14) and use this in the solution of the sensitivity kinematic problem.

8. NUMERICAL RESULTS

As a first step in investigating the accuracy and potential of the developed multi-length scale methodology, we address here a sample design problem referring to a material point. Consider a specimen made of 99.987% pure polycrystalline f.c.c aluminum. The material properties for f.c.c aluminum are specified in [1]. The present design simulator, which is a material point simulator, is used to identify the applied strain rate on a universal material testing machine when given test data that are stresses at particular test times. The objective function for the gradient optimization problem is stated as follows:

$$\min_{\dot{\gamma}} \mathcal{F}(\dot{\gamma}) = \frac{1}{N_s} \sum_{i=1}^{N_s} (\sigma_i(\dot{\gamma}) - \sigma_i^{desired})^2 \quad (26)$$

where N_s is the number of sampling points, and $\sigma_i^{desired}$ is the stress response at different times obtained by a tension process with a strain rate of 0.01. The initial guess strain rate is taken as 0. The stress responses at various intermediate solutions are shown in Fig. 4. The progress of the optimization problem is described by the objective function in Fig. 5. The converged solution corresponded to a strain rate of $9.63E-03$.

ACKNOWLEDGMENTS

This was funded by the Computational Mathematics program of the Air Force Office of Scientific Research (grants F49620-00-1-0373 and FA9550-04-1-0070) and by the National Science Foundation (grant DMI-0113295). This research was conducted using the resources of the Cornell Theory Center.

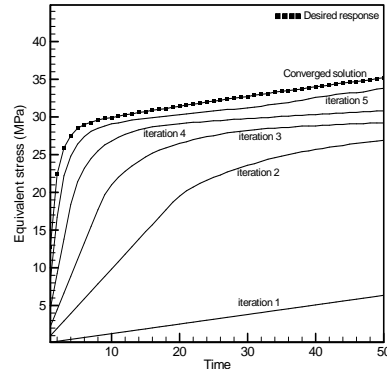


FIGURE 4. The different stress responses obtained at intermediate solutions of the optimization problem.

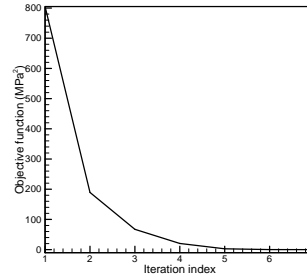


FIGURE 5. Variation of the objective function with optimization iterations for the optimization problem.

REFERENCES

1. S. Ganapathysubramanian and N. Zabarar, *Int. J. Plasticity* submitted (2003).
2. S. Ganapathysubramanian and N. Zabarar, Multi-length scale continuum sensitivity analysis for deformation processes. *In preparation*.
3. N. Zabarar, S. Ganapathysubramanian and Q. Li, *Int. J. Mech. Sciences* **45**,325–358 (2003).
4. S. Ganapathysubramanian and N. Zabarar, *Int. J. Solids Struct* **41**/7,2011–2037 (2004).
5. B. L. Adams, A. Henrie, B. Henrie, M. Lyon, S. R. Kalidindi and H. Garmestani, *J. Mech. Phys. Solids* **49**,1639–1663 (2001).
6. S. R. Kalidindi, C. A. Bronkhorst and L. Anand, *J. Mech. Phys. Solids* **40**,537–569 (1992).
7. S. Ganapathysubramanian and N. Zabarar, *Comput. Methods Appl. Mech. Engrg* submitted (2003).
8. A. Kumar and P. R. Dawson, *Comput. Methods Appl. Mech. Engrg* **153**,259–302 (1997).
9. S. Acharjee and N. Zabarar, *Comput. Methods Appl. Mech. Engrg* submitted (2004).
10. S. Ganapathysubramanian and N. Zabarar, *Int. J. Numer. Methods Engrg* **55**,1391–1437 (2002).
11. H. J. Frost and M. F. Ashby, *Deformation Mechanism Maps*, Pergamon press, New York.